Eur. Phys. J. B (2018) 91: 307
https://doi.org/10.1140/epjb/e2018-90390-3

THE EUROPEAN PHYSICAL JOURNAL B

Regular Article

Breakdown of a topological transition in two-dimensional spin-ice due to geometry effects

Maria Victoria Ferreyra[1] and Santiago A. Grigera[1,2,a]

[1] Instituto de Física de Líquidos y Sistemas Biológicos, UNLP-CONICET, La Plata 1900, Argentina
[2] SUPA, School of Physics and Astronomy, University of St Andrews, North Haugh, St Andrews KY16 9SS, UK

Received 14 June 2018 / Received in final form 25 August 2018
Published online 5 December 2018

Abstract. We investigate the topological transition that takes place in spin-ice systems when a polarising field is applied along a principal axis. In particular, we analyse a two dimensional spin-ice model; we find that the topological transition is strongly affected by geometrical constraints in the shape of the sample, and that in the case where the dimension perpendicular to the field is much smaller than the longitudinal one, i.e. in the quasi-1D *spin-ice-ladder* limit, it splits into a series of first-order phase transitions characterised by sharp spikes in the specific heat and susceptibility.

1 Introduction

Spin-ice is a class of magnetic material where rich behaviour arises from a simple and straightforward origin: the local enforcement of the ice rules [1–3]. These stipulate that for each tetrahedron of the pyrochlore lattice, two spins should point in, and two should point out along the local body-centred diagonal axes. This translates, in a course grained picture, to a vanishing of the divergence of the spin field at a local level [4]. This local constraint gives rise to an extensively degenerate ground state, and to a whole variety of emergent behaviour, notably, artificial magnetostatics [5], where excitations from the ice-rule behave as magnetically charged particles. This is not to say that there is no interesting behaviour even if the ice-rules are strictly enforced. The ice rule applied to every tetrahedron means the magnetisation of each (1 0 0) plane is the same, and hence a topological quantity that can only be changed by a system-wide move [6]. As pointed out by Jaubert and coworkers [7,8], this local constraint can give rise to a topological transition of the Kasteleyn type [9–11]. The configurations that make up the ice-rule manifold usually have different magnetisations, however, if a field is applied along [1 0 0], the degeneracy can be entirely eliminated without violating the ice rule. If the temperature is low enough that no excitation from the ice rule manifold is permitted, i.e. no individual spin-flips, the lowest energy excitation is a string of flipped spins extending from one side of the system to the other. These strings of negative magnetisation cost Zeeman energy, but are entropically favourable. The line in the field–temperature plane where these excitations become favourable is the Kasteleyn transition, characterised by an asymmetric nature, appearing to be first order on one side and continuous on the other. This topological transition between a single and a multiple connected system has been shown to occur both in three-dimensional [7,12] and two-dimensional spin-ice [13].

The mechanism by which this transition takes place – the proliferation of sample-length spanning strings – make it extremely anisotropic in nature. This type of transition not only requires special treatment when performing a finite-size scaling analysis [14] but can also be prone to fundamental changes in its nature due to geometrical constraints on the sample shape [15]. The purpose of this work is to investigate the nature of the Kasteleyn transition in spin-ice systems under different geometries. We will show that in the case of thin, semi-infinite samples, oriented along the field direction, the Kasteleyn transition is replaced by a series of first-order phase transitions characterised by very sharp delta-like spikes in the specific heat.

2 Model and simulation methods

For this work we have chosen the model introduced in reference [13]. This is a simple two-dimensional ice model that has the advantage that it has the same Ising quantization axis for every spin. We consider magnetic moments on a two-dimensional square lattice such that $\vec{\mu}_i = \sigma_i \vec{\mu}$, where $\sigma_i = \pm 1$ is an Ising variable on lattice site i, and the moment μ points along one of the principal axes of the lattice (see inset of Fig. 2). The Hamiltonian is given by

$$H = \sum_{ij} J_{ij}\sigma_i\sigma_j - h\sum_i \sigma_i, \qquad (1)$$

[a] e-mail: sag2@st-and.ac.uk

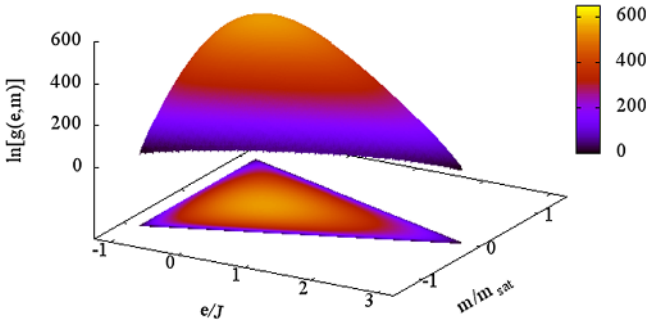

Fig. 1. Logarithm of the density of states $g(e, m)$ as a function of the energy per site e and the normalized magnetisation, m/m_{sat} calculated using the the Wang–Landau algorithm for a system size of 8×100 unit cells. The projection to the e–m plane reveals the ground state is composed of a large number of states with same energy and different magnetisation.

where i and j label the sites of the lattice, and $h = \vec{\mu} \cdot \vec{H}$, with $\vec{H}$ the externally applied magnetic field. In all cases considered here, the field is kept purely longitudinal. The exchange interaction J_{ij} is given by

$$J_{ij} = \begin{cases} J & \mathbf{r}_j = \mathbf{r}_i + \hat{\mathbf{x}}; \\ -J & \mathbf{r}_j = \mathbf{r}_i + \hat{\mathbf{y}}; \\ -J & \mathbf{r}_i = n\hat{\mathbf{x}} + m\hat{\mathbf{y}} \quad (n+m \text{ odd}) \\ & \quad \text{and } \mathbf{r}_j = \mathbf{r}_i + \hat{\mathbf{x}} + \hat{\mathbf{y}}; \\ -J & \mathbf{r}_i = n\hat{\mathbf{x}} + m\hat{\mathbf{y}} \quad (n+m \text{ even}) \\ & \quad \text{and } \mathbf{r}_j = \mathbf{r}_i - \hat{\mathbf{x}} + \hat{\mathbf{y}}; \\ 0 & \text{otherwise}, \end{cases} \tag{2}$$

As shown in the inset of Figure 2, this is a simple Ising model on a checkerboard lattice with mixed ferromagnetic (vertical and diagonal bonds) and antiferromagnetic (horizontal bonds) interactions of the same magnitude. As shown in [13], this system has an ice-like ground state with Lieb's residual entropy and undergoes a Kasteleyn transition in the field–temperature plane that is well described by equating the energy and entropic contributions: $T_c = 2h/(k_{\text{B}} \ln 2)$. This transition is characterised by a one-sided drop of the magnetisation, and an asymmetric lambda-like peak in the susceptibility.

For our simulations we have performed Monte Carlo simulations using the Metropolis and Wang–Landau [16] algorithms. In both cases we used a single-spin-flip algorithm on systems of varied geometric configurations as described later. We used the Wang–Landau algorithm to determine the density of states g. We labeled the states according to their energy E_i and magnetisation M_i. For normalization we used the condition $\sum_{E_i,M_i} g(E_i, M_i) = 2^N$, where N is the total number of spins of the system. The modification factor changed from $\ln(f_0) = 1$ to $\ln(f_{\text{final}}) = 10^{-9}$.

3 Results

In order to investigate the effects of the system shape on the thermodynamic quantities, we calculate the density of states $g(E, M)$ for different rectangular lattice sizes of

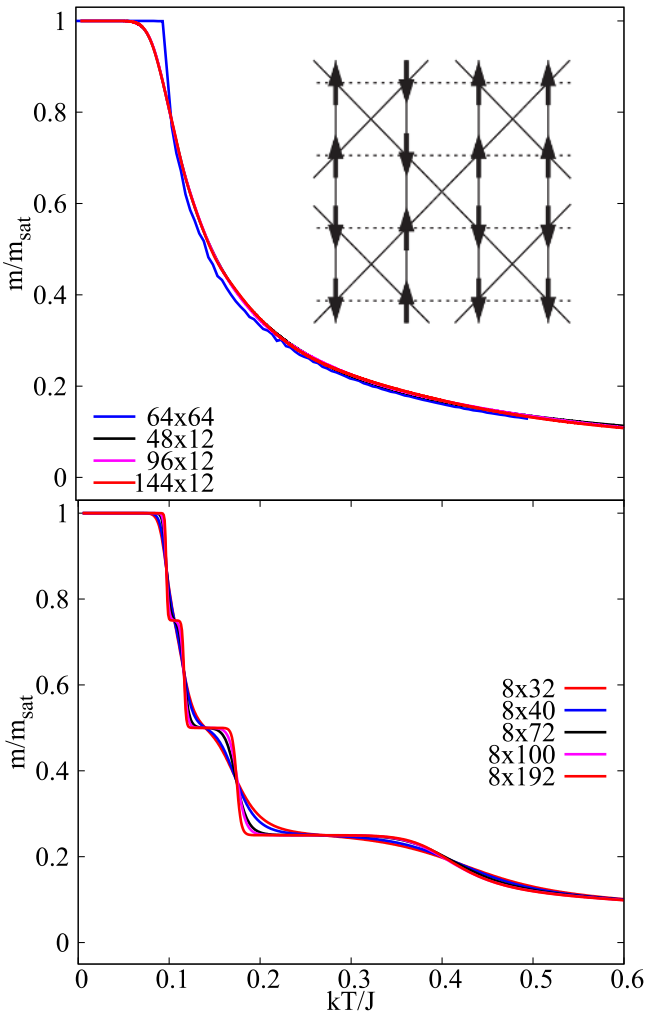

Fig. 2. Relative magnetisation versus temperature with $h/J = 0.0336$ for different lattice sizes and shapes. L' and L are the lattice sizes in the directions perpendicular and parallel to the field, respectively. The upper panel shows a square lattice and lattices with $L' > L$. Both cases show similar behavior: at low temperatures, the system is completely saturated and the magnetisation decreases continuously as the strings enter the system. In the plot it is not possible to resolve the difference between the different curves with $L' > L$. The bottom panel shows the magnetisation with $L' < L$; here the decrease from saturation happens at a series of well-defined steps. The inset shows a schematic view of the lattice, with ferromagnetic bonds represented by solid lines and antiferromagnetic bonds by dotted lines.

$L \times L'$ by using the Wang–Landau algorithm. Figure 1 shows a typical result for the logarithm g as a function of the energy per spin, $e = E/N$ and magnetisation per spin, $m = M/N$ for a rectangular sample of 8×100 unit cells. As expected for a frustrated system, the density of states is asymmetric along the energy axis and symmetric along m. The projection into the e–m plane shows a triangular shape, with a well-defined magnetisation state at maximum energy and a wide base at the ground energy marking the degeneracy of the ice state.

From $g(E, M)$ one can easily calculate the relevant thermodynamic quantities by using the expression for

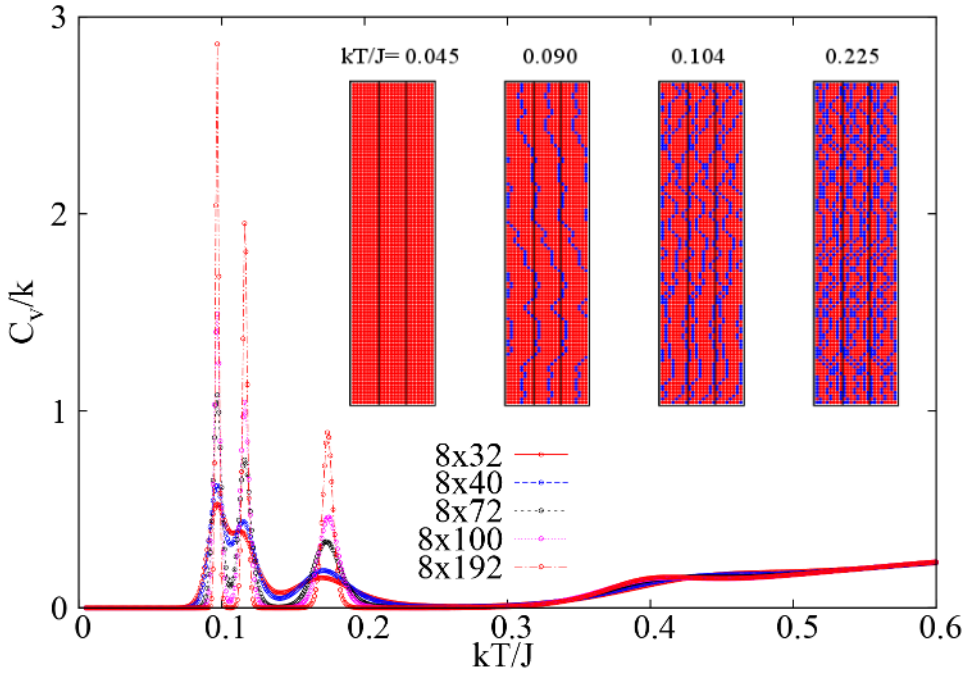

Fig. 3. Specific heat curves calculated for different lattice sizes with $h/J = 0.0336$. The figure shows the sharp peaks marking the successive transitions into which the Kasteleyn transition is broken down. *Inset*: Snapshots for different temperature values, for a 8×100 unit cell system size. Black lines mark the simulation box, which has been repeated to the left and right in order to make more explicit the periodic boundary conditions. The strings of downward-pointing spins (blue dots) enter the sample one by one as the temperature increases.

the partition function in the magnetic isothermal–isobaric ensemble:

$$\mathcal{Z} = \sum_{E,M} \delta(E, M) e^{-\beta(E - Mh)} \tag{3}$$

from which all relevant thermodynamic quantities can be extracted.

Figure 2 shows the magnetisation calculated from the Wang–Landau simulations. The upper panel shows the result for a square-shaped lattice ($L \times L$) together with lattices of $L' > L$, where L' is the direction perpendicular to the field. The magnetisation is shown as a function of temperature at a fixed value of $h/J = 0.0336$ (which corresponds to a longitudinal field of 0.05 T in a system with $\mu = 1\mu_B$ and $J = 1$ K). At low temperatures the system is in the singly connected phase, and in the absence of excitations is fully polarized ($M/M_{sat} = 1$). As the temperature is raised, the entropic contribution to the free energy from a string excitation becomes increasingly higher till it overcomes the energetic loss and strings of negative magnetisation spanning the whole sample pierce the system. This is seen as a sharp continuous decrease in the magnetisation. Finite size effects are quite mild in this case; the main effect is a rounding off of the transition, where instead of a decrease in M with a divergent slope: the more the departure from saturation is smoother, the smaller the size of the sample. The lower panel shows the magnetisation under the same conditions but for samples with $L > L'$, that is samples where the length along the field direction is much longer than in the perpendicular direction. In this case the scenario is drastically changed by finite size effects: the continuous decrease of M/M_{sat} as the temperature is raised above a transition is instead replaced by a series of sharp steps, which become sharper the longer the sample is along the field direction. When the specific heat is calculated (see Fig. 3), it is seen that these steps in magnetisation correspond to delta-like peaks in the specific heat that become sharper as the sample size is increased along the field direction. The Kasteleyn transition has been split into a series of transitions that, as we will see later, are first order in nature.

This type of behaviour has been observed to occur in dimer models [15]. The origin of this change is found in the entropic contribution of the strings to the system. In an infinite case, once the entropic condition is favourable for strings to exist, there is a rush of strings that pierce through the sample and which increase gradually in number as the temperature is raised. There are two different scenarios when one of the directions is limited: if we limit the direction parallel to the field, L, we make the strings shorter, but we leave essentially unchanged the way in which they interact with each other, while if we reduce the direction perpendicular to the field, L', we force the strings to see each other even at extremely low densities. This interaction reduces the number of possible configurations of two strings compared with two independent strings. If L' is sufficiently small then the introduction of each single string is accompanied by an entropic change which is different in each case; the condition of entropic gain versus energy loss is then different for each string, and the temperature is thus split into separate temperatures for every time a string enters into the sample. The configurations between peaks in the specific heat are shown in the

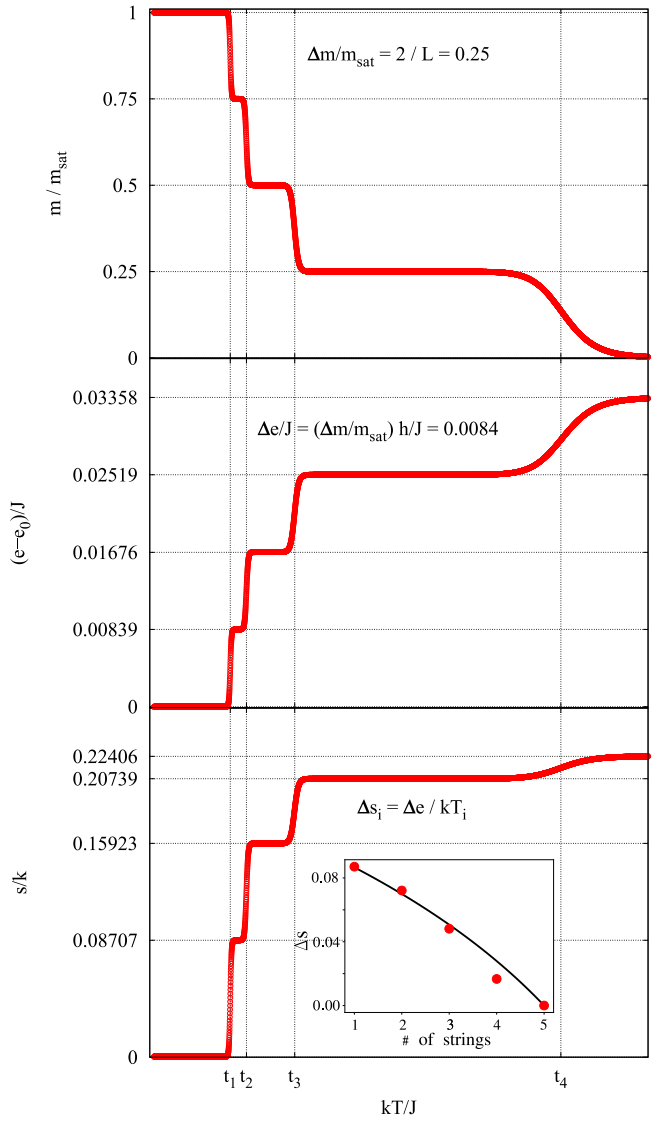

Fig. 4. Magnetisation, energy and entropy per spin versus temperature calculated for $h/J = 0.0336$ using the subset of non-defects configurations. t_1, t_2, t_3 and t_4 correspond with the position of the peaks in the specific heat curves, 0.0969, 0.1164, 0.1744 and 0.4961, respectively. In absence of defects, Δe and Δm do not change as the strings appear in the lattice, but ΔS is not constant due to the interaction between strings. The inset shows ΔS as a function of the number of strings present in the system (red dots) compared with the expression obtained in equation (4) (black line).

inset determined from a Metropolis simulation. Red indicates up-pointing spins and blue down-pointing spins. The sample has been repeated to left and right in order to make explicit the periodic boundary conditions. As seen in the Metropolis snapshots, the low temperature region, below the first peak, is a homogeneous fully saturated sample. As the temperature is raised, a single string spanning the whole length of the sample enters and is accompanied by a peak in the specific heat. Further peaks in the specific heat correspond to further introduction of strings.

This picture can be accounted for in a more quantitative manner. Figure 4 shows the magnetisation, energy and entropy calculated at a fixed field as a function of temperatures with the condition that no violations to the ice-rule occur [17]. The reduced temperatures $t_i = kT_i/J$ mark the entrance of i string defects into the system. As it can be seen in the figure, the entrance of a defect produces a simultaneous jump in the magnetisation (down), the energy (up) and the entropy (up). A more careful inspection shows that while the magnetisation jumps (and consequently the energy jumps) are of the same magnitude in all cases ($\Delta M/M_{\text{sat}} = 0.25(2), \Delta E/J = 0.0084(1)$), the entropy jump $\Delta S/k$ changes substantially as the number of defects increases: 0.08707(5), 0.07214(5), 0.048156(5) and 0.01667(5) (plotted as red dots in the inset). ΔM and ΔE can be straightforwardly calculated: a string of negative magnetisation of length L contributes a change in $m = M/N = 2L/LL' = 2/L'$, where N is the total number of spins. In the case of these simulations, with $L' = 8$, the jump is $\Delta M = 2/8 = 1/4$ which coincides with the simulations. The change in energy, given that there are no violations to the ice rule, is simply the Zeeman energy $\Delta E/J = Mh/J = 2h/JL' = 0.25 \times 0.0336 = 0.0084$ again in coincidence with what is determined from the figure. The change in entropy due to the introduction of the first string is simply $\Delta S_1/k = L \ln 2/LL' = \ln(2)/L' = 0.087$, which coincides well with the first jump. The additional entropy of subsequent strings is decreased by the interaction with the previously existing strings in the sample. An exact calculation of the subsequent jumps involves taking into account the correlation due to closed loops, in a fashion similar to Lieb's determination of the zero-point entropy, but it is possible to obtain a simple estimate that fits well the entropy of the system if the density of strings is not high. Each step in the propagation of a string means flipping one spin of a plaquette from up to down. In the zero density limit there are always two choices – to continue vertically or diagonally – but for a system with $P-1$ strings, the probability that one of these two sites of the plaquette would already have one downward-pointing spin is $p_\downarrow = 1 - (P-1)/L$. The change in entropy ΔS_P after the introduction of an additional string can then be estimated by weighting the number of choices with the probability $p_\downarrow$:

$$\Delta S_P/k = \ln\left(2\left[1 - \frac{P-1}{L}\right]\right). \tag{4}$$

This simple estimate gives the two limits correctly: for $P/L \to 0$, one recovers $\Delta S = \ln 2$ that fits well the $(\infty \times \infty)$ and $(\infty \times L')$ limits (see e.g. [13]) , and for $P - 1 = L/2$, we get the correct value $\Delta S = 0$ since there is no longer any choice of sites to add additional strings. The inset of the lowermost panel of Figure 4 shows a comparison between the entropy jumps observed (red dots) and the estimate given by equation (4). As expected, the estimate works best for a small number of strings.

With the knowledge of ΔE and ΔS, it is straightforward to calculate the t_i at which it is favourable to let a string into the system:

$$\Delta G = \Delta E - T_i \Delta S = 0. \tag{5}$$

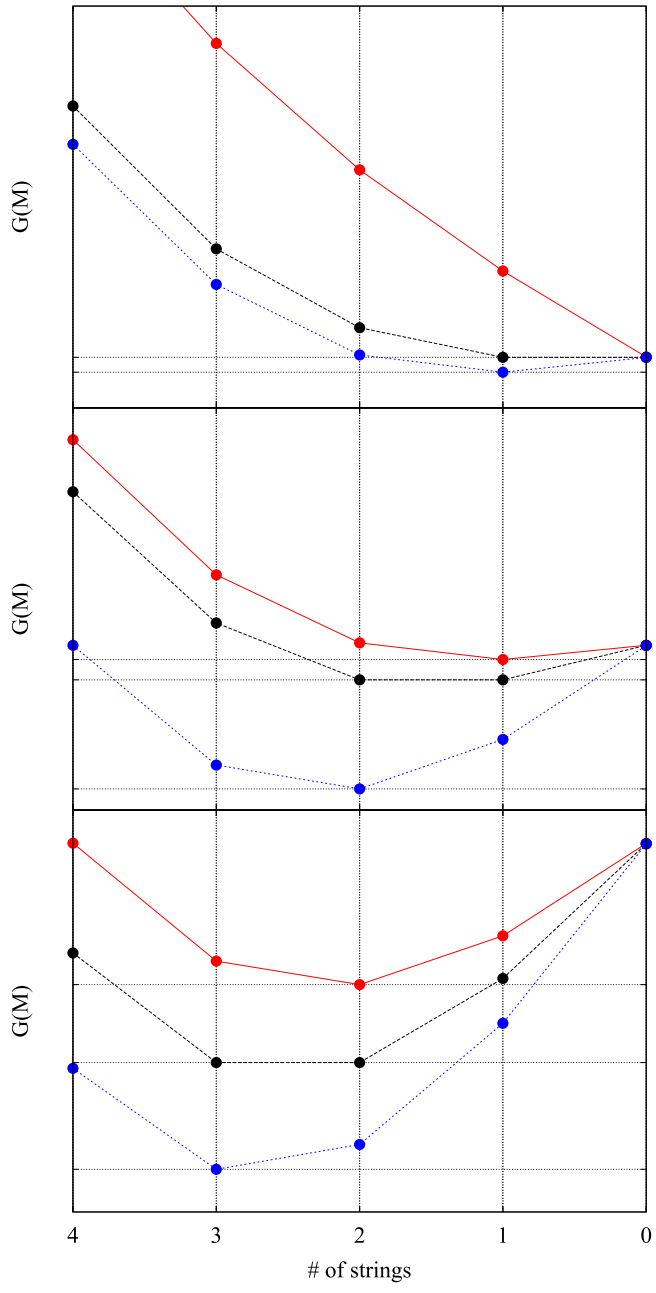

Fig. 5. Free energy $G(M)$ per spin versus magnetisation for different temperature values (indicated in terms of the number of negative strings present in the system). In each panel, the black curve points were calculated at the temperature of the transition T_i. The blue (red) curve corresponds to temperatures above (below) T_i. The minimum of the curve indicates in each case the magnetisation value of the correspondent phase.

Then, from the data in Figure 4,

$$t_1 = \frac{\Delta E/J}{\Delta S_1} = \frac{0.008397(5)}{0.08707(5)} = 0.0964(3), \quad (6)$$

$$t_2 = \frac{\Delta E/J}{\Delta S_2} = \frac{0.008397(5)}{0.072141(5)} = 0.1164(27), \quad (7)$$

$$t_3 = \frac{\Delta E/J}{\Delta S_3} = \frac{0.008397(5)}{0.0481564(5)} = 0.174(6), \quad (8)$$

which are in good agreement with those determined from the simulations (see Fig. 4). The key of the breakdown of the original Kasteleyn transition into a succession of first-order transitions is this straightforwardly linked with the change in ΔS as a function of the number of strings,

The Wang–Landau method provides us an additional valuable information that can be used to determine the nature of the transitions: from the knowledge of $g(E, M)$ it is possible to calculate the free energy of the system as a function of the order parameter (in this case, the magnetisation). Figure 5 shows the Gibbs potential as a function of the magnetisation, calculated from the configurations without defects and for $h/J = 0.0336$. The three panels correspond to the transitions at T_1, T_2 and T_3. In each panel the black curve is calculated at the transition temperature T_i, and the red and blue curves for $T < T_i$ and $T > T_i$, respectively. The magnetisation axes have been labeled in terms of the magnetisation of the system with n strings. In the uppermost panel, the system progresses as the temperature is lowered from a minimum at 0 (no strings) to a minimum at 1 (one string). The black line shows that at the transition both minima are at the same temperature, i.e. it is a first-order phase transition. The discontinuity in the jump of M as a function of the temperature has its origin in the fact that due to the topological constraints, only a discrete number of magnetisation values are allowed, that is those marked by points in the curve, the lines are merely guides to the eyes. This remains true even in the thermodynamic limit of a semi-infinite sample along the field direction. An identical description applies to the other two transitions showed in the panels.

4 Conclusions

We investigated the topological transition that takes place in spin-ice systems when a polarising field is applied along a principal axis. In particular, we have analysed the two dimensional spin-ice model presented in reference [13] which has the advantage that it has the same Ising quantization axis for every spin. We found that the topological Kasteleyn transition is strongly affected by geometrical constraints in the shape of the sample and that in the case where the dimension perpendicular to the field is much smaller than the longitudinal one ($L < L'$), the Kasteleyn transition splits into a series of transitions characterised by sharp spikes in the specific heat and susceptibility. The limit towards infinite number of particles with a finite length in one direction (a *quasi-1D spin-ice ladder*) gives two completely different scenarios regarding the type and number of transitions observed in the system: a Kasteleyn transition in one case ($\infty \times L'$), and a series of first-order transitions in the other ($L \times \infty$). Taking the thermodynamic limit with both L and L' going to infinity also gives rise to different behaviour depending on the ratio between these two lengths In the case of $L > L'$ the approach towards the limit shows the usual behaviour of a continuous transition, while in the case of $L < L'$ it is characterised by the presence of a series of individual transitions with the number of steps that become denser as N

is increased. We expect that this type of behaviour can be observed experimentally in the case of artificial spin-ice systems [18], and particularly in the case of colloidal systems where bespoke vertex energies can be tuned [19–21].

We are pleased to acknowledge useful discussions with Rodolfo Borzi. This work was supported by CONICET (Argentina) and by ANPCYT (Argentina) via grant PICT-2013-2004.

Author contribution statement

M.V.F. wrote the code, run the simulations and prepared the figures. S.A.G. conceived the project and wrote the article. Both authors are responsible for the analysis of the results.

References

1. S.T. Bramwell, M.J.P. Gingras, Science **294**, 1495 (2001)
2. R. Moessner, Can. Phys. **79**, 1283 (2001)
3. C. Lacroix, P. Mendels, F. Mila, in *Introduction to Frustrated Magnetism: Materials, Experiments, Theory* (Springer Science & Business Media, 2001), Vol. 164
4. C.L. Henley, Annu. Rev. Condens. Matter Phys. **1**, 179 (2010)
5. C. Castelnovo, R. Moessner, S.L. Sondhi, Nature **451**, 42 (2008)
6. R. Moessner, J. Chalker, Phys. Rev. B **58**, 12049 (1998)
7. L.D.C. Jaubert, J.T. Chalker, P.C.W. Holdsworth, R. Moessner, Phys. Rev. Lett. **100**, 067207 (2008)
8. L.D. Jaubert, Topological Constraints and Defects in Spin Ice, Ph.D. thesis, Ecole normale supérieure de Lyon, 2009
9. P.W. Kasteleyn, J. Math. Phys. **4**, 287 (1963)
10. J. Nagle, Proc. Natl. Acad. Sci. **70**, 3443 (1973)
11. J.F. Nagle, C.S. Yokoi, S.M. Bhattacharjee, Phase Trans. **13**, 236 (1989)
12. M. Baez, R. Borzi, J. Phys.: Condens. Matter **29**, 055806 (2016)
13. S. Grigera, C. Hooley, J. Phys. Commun. **2**, 085004 (2018)
14. K. Binder, J.-S. Wang, J. Stat. Phys. **55**, 87 (1989)
15. S.M. Bhattacharjee, J.F. Nagle, D.A. Huse, M.E. Fisher, J. Stat. Phys. **32**, 361 (1983)
16. F. Wang, D.P. Landau, Phys. Rev. Lett. **86**, 2050 (2001)
17. M.V. Ferreyra, G. Giordano, R.A. Borzi, J.J. Betouras, S.A. Grigera, Eur. Phys. J. B **89**, 51 (2016)
18. C. Nisoli, R. Moessner, P. Schiffer, Rev. Mod. Phys. **85**, 1473 (2013)
19. A. Libál, C. Reichhardt, C.J.O. Reichhardt, Phys. Rev. Lett. **97**, 228302 (2006)
20. Y. Han, Y. Shokef, A.M. Alsayed, P. Yunker, T.C. Lubensky, A.G. Yodh, Nature **456**, 898 (2008)
21. A. Ortiz-Ambriz, P. Tierno, Nat. Commun. **7**, 10575 (2016)